

**The following resources related to this article are available online at [www.sciencemag.org](http://www.sciencemag.org) (this information is current as of November 26, 2009):**

**Updated information and services**, including high-resolution figures, can be found in the online version of this article at:

<http://www.sciencemag.org/cgi/content/full/279/5353/1018>

This article **cites 8 articles**, 1 of which can be accessed for free:

<http://www.sciencemag.org/cgi/content/full/279/5353/1018#otherarticles>

This article has been **cited by** 98 article(s) on the ISI Web of Science.

This article has been **cited by** 2 articles hosted by HighWire Press; see:

<http://www.sciencemag.org/cgi/content/full/279/5353/1018#otherarticles>

This article appears in the following **subject collections**:

Atmospheric Science

<http://www.sciencemag.org/cgi/collection/atmos>

Information about obtaining **reprints** of this article or about obtaining **permission to reproduce this article** in whole or in part can be found at:

<http://www.sciencemag.org/about/permissions.dtl>

35. J. I. Martinez, *Palaeogeogr. Palaeoclimatol. Palaeoecol.* **112**, 19 (1994); ———, P. DeDeckker, A. R. Chivas, *Mar. Micropaleontol.* **32**, 311 (1997).
36. D. P. Schrag, G. Hampt, D. W. Murray, *Science* **272**, 1930 (1996).
37. The along-track scanning radiometer (ATSR) data are supplied by the European Space Agency and have been analyzed by the Rutherford Appleton Laboratory, UK.

38. We thank I. Ward for assistance with coral sample preparation and mass spectrometry; S. Anker, S. Vellacott, P. Walbran, and W. Hantoro for help with collecting corals; and W. Beck, D. Schrag, B. Linsley, D. Battisti, and K. Trenberth for valuable discussions. Financial support was provided by the Australian National Greenhouse Advisory Committee.

3 October 1997; accepted 23 December 1997

## Simulated Increase of Hurricane Intensities in a CO<sub>2</sub>-Warmed Climate

Thomas R. Knutson,\* Robert E. Tuleya, Yoshio Kurihara

Hurricanes can inflict catastrophic property damage and loss of human life. Thus, it is important to determine how the character of these powerful storms could change in response to greenhouse gas-induced global warming. The impact of climate warming on hurricane intensities was investigated with a regional, high-resolution, hurricane prediction model. In a case study, 51 western Pacific storm cases under present-day climate conditions were compared with 51 storm cases under high-CO<sub>2</sub> conditions. More idealized experiments were also performed. The large-scale initial conditions were derived from a global climate model. For a sea surface temperature warming of about 2.2°C, the simulations yielded hurricanes that were more intense by 3 to 7 meters per second (5 to 12 percent) for wind speed and 7 to 20 millibars for central surface pressure.

Greenhouse gas-induced climate warming could affect hurricanes in a number of ways, including changing their intensity (1, 2), frequency (3–5), and locations of occurrence. Given the potential for catastrophic damage and loss of life from these storms, any such changes could have important societal consequences. In this study, we examine only the question of possible changes in storm intensity due to climate warming.

Theoretical models of hurricane intensity predict that the maximum potential intensity (MPI) of hurricanes will increase in a warmer climate (1, 2), although these techniques, which are based on thermodynamical considerations, contain many assumptions and caveats (2, 6, 7). Global climate models attempt to simulate the climate, including tropical storm-like features, by integrating dynamical and thermodynamical equations in three dimensions. To date, global models have provided suggestive, but not highly convincing, indications of increased hurricane intensities in a warmer climate (3, 4). However, the coarse resolution of these global models precludes their simulation of realistic hurricane structure. A 1995 assessment by the Intergovernmental Panel on Climate Change (8) concludes that “. . . it is not possible to say whether the . . . maximum intensity of tropical cyclones will change” because of

increased greenhouse gas concentrations. In the present study, the relation between hurricane intensity and climate change was explored with a regional, high-resolution, hurricane prediction model. We focused on the northwest tropical Pacific region, where the strongest typhoons (the term used in the northwestern Pacific for hurricanes) are observed in the present climate.

In our case study approach, we selected 51 tropical storm cases from a control climate simulation of a global climate model and 51 cases from a high-CO<sub>2</sub> climate simulation (9). The global model used was the Geophysical Fluid Dynamics Laboratory (GFDL) R30 coupled ocean-atmosphere climate model (10–12), which has resolution of about 2.25° latitude by 3.75° longitude. For the high-CO<sub>2</sub> cases, we selected storms from years 70 to 120 of a +1%-per-year CO<sub>2</sub> transient experiment, corresponding to CO<sub>2</sub> increases ranging from a factor of 2.0 to 3.3. Tropical storm-like features (weaker and much broader than in real-world storms) have previously been analyzed in an R30 global atmospheric model very similar to that used here (5, 13). The selected storm cases were then rerun as 5-day “forecast” experiments with the use of the high-resolution GFDL Hurricane Prediction System (14), which is currently used at the U.S. National Centers for Environmental Prediction (NCEP). This model has a maximum resolution in the storm region of 1/6° or about 18 km (15). Before beginning each hurricane model simulation, the crudely resolved global model storm (but

not the background environment) was filtered from the global model fields and replaced by a more realistic initial vortex (16, 17). This initial vortex replacement procedure is analogous to that used for operational hurricane prediction at NCEP. The storm intensity distributions of the control and high-CO<sub>2</sub> case studies were then compared. Sea surface temperatures (SSTs) were held fixed during the hurricane model experiments. The SSTs and initial environmental

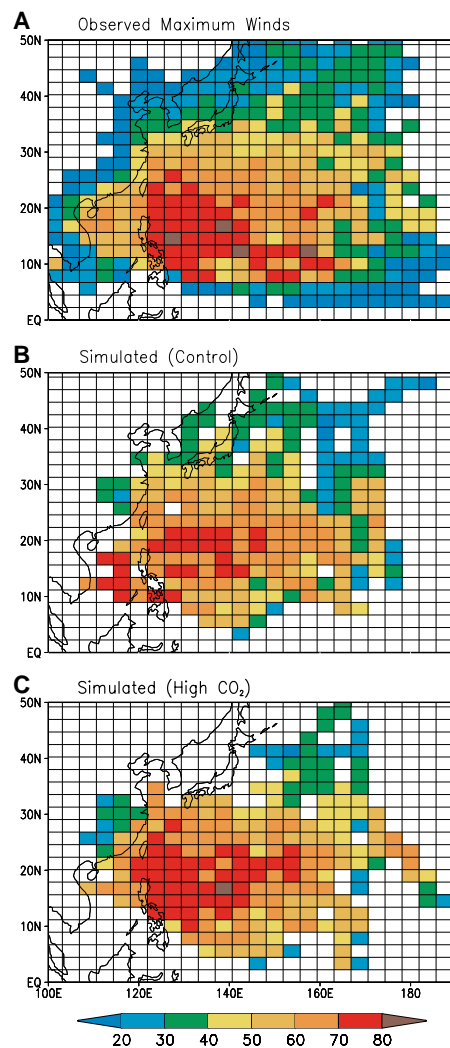


**Fig. 1.** Geographical distribution of the maximum surface wind speeds (in meters per second) observed during 1971–1992 (A) and simulated (B and C) for tropical storms in the northwest Pacific basin. Observations are from the Joint Typhoon Warning Center (Guam) as compiled by C. J. Neumann in 1993, available from the National Center for Atmospheric Research at [www.scd.ucar.edu/dss](http://www.scd.ucar.edu/dss) (ds824.1). The simulated distributions are based on 71 case studies each under control (B) and high-CO<sub>2</sub> (C) conditions; results from 20 preliminary cases under each condition (9) were included in order to increase spatial coverage. Blank (white) regions denote areas where no tropical storms were reported during 1971–1992 (A) or none occurred in the case studies [(B) and (C)].

Geophysical Fluid Dynamics Laboratory/National Oceanic and Atmospheric Administration, Post Office Box 308, Princeton, NJ 08542, USA.

\*To whom correspondence should be addressed. E-mail: [tk@gfdl.gov](mailto:tk@gfdl.gov)

conditions used for the regional hurricane model simulations were derived from the global climate model. The sensitivity of climate to CO<sub>2</sub> concentrations in a hypothetical global version of the hurricane

model could be different from that of the R30 global climate model, but is not investigated here.

The spatial distribution and magnitude of the wind speeds in the control cases (Fig. 1B) are fairly realistic in comparison to observed conditions (Fig. 1A). In particular, there is a decrease in maximum intensities over higher latitudes (with cooler SSTs), near the equator, and over land regions. One shortcoming of our simulations is that wind speeds in the strongest storms appear to be slightly underpredicted in the control cases (Fig. 1B) as compared with actual observations (Fig. 1A). This underprediction of high wind speeds for intense storms is a known bias of the hurricane model, although the model nonetheless simulates surface pressure minima at least as low as the observed record (870 mb). The high-CO<sub>2</sub> distribution (Fig. 1C) has more areas of very intense (>70 m/s) wind speeds than does the control distribution (Fig. 1B), which suggests a modest increase in maximum surface winds in response to CO<sub>2</sub>-induced warming.

nificant at the 90% confidence level, with a probability of obtaining such a result by chance of 0.059. A comparison of the storm intensities simulated by the global climate model for these case studies (20) indicates that the high-CO<sub>2</sub> cases were slightly more intense than the control cases, but the difference is not statistically significant according to the KS test.

In terms of minimum surface pressure, there is considerable scatter among the storm cases (Fig. 3). In both the control and high-CO<sub>2</sub> sets of storm cases, there are several relatively weak storms (>920 mb) even at high SSTs. The median value for the high-CO<sub>2</sub> cases shown in Fig. 3 is lower (more intense) than the control by 6.6 mb. However, the overall pressure distribution for the high-CO<sub>2</sub> cases is not significantly lower than the control distribution, according to the KS test. Nonetheless, the strongest storms occur in the high-CO<sub>2</sub> cases, with five storms intensifying to 860 mb or below, as compared to one storm in the control cases. Thus, the envelope of intensities appears to expand to include lower pressures (that is, higher storm intensities) for higher SSTs, as shown schematically by the dark curve. This result is consistent with theoretical calculations (1, 2) suggesting an increase in the maximum attainable storm intensity in a CO<sub>2</sub>-warmed climate.

Application of the KS test to the available storm cases (21) at each hour of the 120-hour simulations (Fig. 4A) indicated that the tendency for the high-CO<sub>2</sub> storms to be more intense than the control storms is statistically significant, although not at all times during the 120-hour period. As a measure of the behavior of the more intense storms, we compared the value of the fifth lowest central pressure (~90th percentile intensity) for each hour among the available storm cases for high CO<sub>2</sub> and for the

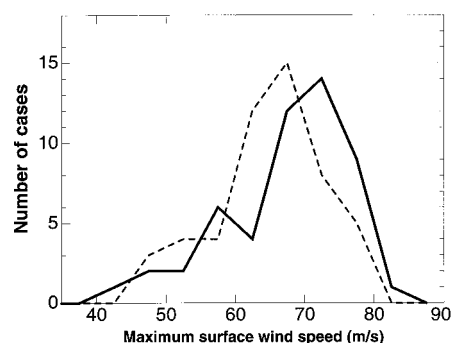


**Fig. 2.** Frequency distribution of maximum surface wind speeds obtained from the hurricane model in 51 case studies each from control (dashed line) and high-CO<sub>2</sub> (solid line) conditions.

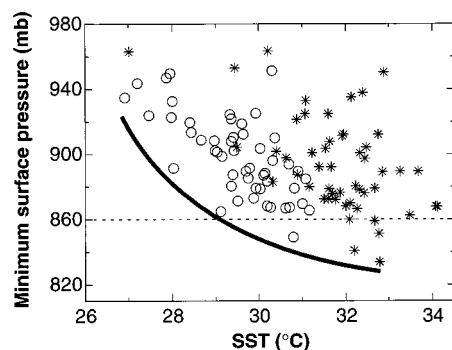


**Fig. 3.** Scatter plot of minimum surface pressure versus local SST obtained from the hurricane model in 51 case studies each under control (circles) and high-CO<sub>2</sub> (asterisks) conditions. The dark curve is drawn to schematically illustrate an expanding envelope of attainable surface pressures with increasing SST. The dashed line indicates the 860-mb level discussed in the text.

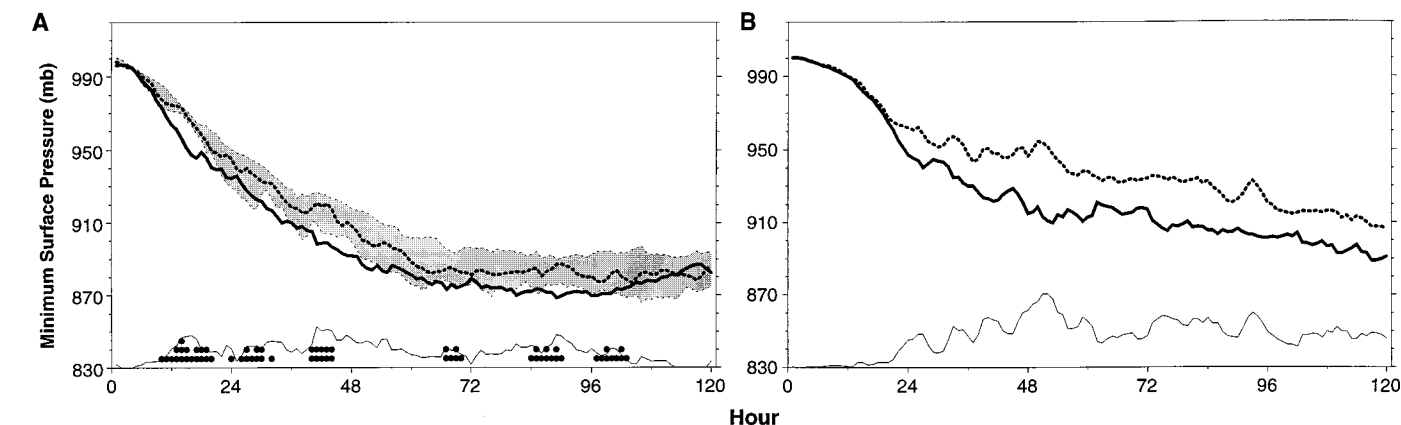


**Fig. 4. (A)** Dark lines show the fifth strongest storm intensity for each hour under control (dashed) or high-CO<sub>2</sub> (solid) conditions; shading depicts 95% confidence intervals for control conditions. Small circles (one to three rows) indicate periods when the high-CO<sub>2</sub> distribution is significantly lower than the

control distribution at the 0.1, 0.05, or 0.01 levels, respectively, according to a KS test. **(B)** Central surface pressure for control (dark dashed line) and high-CO<sub>2</sub> (dark solid line) idealized experiments. Difference curves [light solid lines in (A) and (B)] are offset by +830 mb.

control (Fig. 4A). The high-CO<sub>2</sub> curve generally lies below the control curve, and at times lies below the 95% confidence limit (22, 23) for the control, indicating that the most intense storms in the high-CO<sub>2</sub> case studies tend to be more intense than those in the control cases. A smaller and less statistically distinct change is seen in the medians of the central pressure distributions (20). Although the CO<sub>2</sub>-induced storm intensification is not statistically significant at all times, the sign of the intensity change indicates stronger storms in the warmer climate for virtually the entire 120-hour period. The increase in intensity of the fifth strongest (~90th percentile intensity) storm is about 10 mb for surface pressure and 3 m/s (5%) for wind speed (20).

As a sensitivity test, the hurricane model simulations for all of the control and high-CO<sub>2</sub> case studies were repeated without the use of the initial vortex replacement procedure. The results (20) show a somewhat stronger signal than that shown in Fig. 4A, indicating that the increased storm intensity in the warmer climate suite is not likely to be an artifact of the vortex replacement procedure.

As an alternative to the case studies, a more idealized approach was used in which an initial storm was embedded in an otherwise uniform easterly flow (5 m/s). The SST, temperature, and moisture fields were derived (24) from area averages for the northwest tropical Pacific from the control and high-CO<sub>2</sub> runs of the climate model (from July through November, 8° to 26°N, 124° to 161°E). The increase in SST in the high-CO<sub>2</sub> climate was 2.2°C, compared with an increase of over 5°C in the upper troposphere. The surface pressure time series (Fig. 4B) indicate that the high-CO<sub>2</sub> case is roughly 20 mb more intense than the control; the increase in maximum wind speeds (20) is about 7 m/s (12%). Typical changes of 15 to 20 mb were obtained with background easterly flows varying from 0 to 7.5 m/s (20). It has recently been suggested (2) that in a CO<sub>2</sub>-warmed climate, any intensification of hurricanes due to increased SST would be moderated by more stable lapse rates, such as those simulated in CO<sub>2</sub>-increase experiments using the global climate model. By design, our idealized and case study results include this moderating effect of a more stable tropospheric lapse rate (see above). Although the processes leading to more intense storms under high-CO<sub>2</sub> conditions are not fully understood, we note that both the domain-averaged surface evaporation and the near-storm environmental convective available potential energy (CAPE) are enhanced in the high-CO<sub>2</sub> cases, with the CAPE increasing despite the more stable tropospheric lapse rate under high CO<sub>2</sub> conditions.

Our simulation results can be compared with theoretical estimates of the MPI of hurricanes that were obtained with the same time-mean thermodynamic profiles as our idealized simulations. Using Emanuel's method (6), we obtained an intensity increase of 23 mb and 10 mb, assuming thermodynamically reversible or pseudoadiabatic ascent of air parcels, respectively. With Holland's method (7), we obtained an intensity increase of 18 mb. Thus, the impact of CO<sub>2</sub>-induced warming on hurricane intensity as estimated with the theoretical methods is comparable to our simulation results.

Using both a case study and an idealized approach, we find that CO<sub>2</sub>-induced warming leads to more intense hurricanes (that is, typhoons) in the northwest Pacific basin. Our study does not address a number of important issues, such as the effect of the storm itself on the local SST, uncertainties in air-sea exchange processes (2, 25), sensitivity to model resolution or model physics, and applicability to other tropical cyclone basins. However, we are encouraged by the fact that with the present simulation approach, a reasonable spatial distribution and magnitude of storm intensities can be simulated for the northwest Pacific basin and that our CO<sub>2</sub> sensitivity results are in reasonable agreement with calculations made with theoretical techniques (6, 7).

## REFERENCES AND NOTES

1. K. A. Emanuel, *Nature* **326**, 483 (1987).
2. A. Henderson-Sellers *et al.*, *Bull. Am. Meteorol. Soc.*, in press.
3. R. J. Haarsma, J. F. B. Mitchell, C. A. Senior, *Clim. Dyn.* **8**, 247 (1993).
4. L. Bengtsson, M. Botzet, M. Esch, *Tellus* **48A**, 57 (1996).
5. A. J. Broccoli and S. Manabe, *Geophys. Res. Lett.* **17**, 1917 (1990).
6. K. A. Emanuel, *J. Atmos. Sci.* **43**, 585 (1986); *ibid.* **45**, 1143 (1988); *ibid.* **52**, 3969 (1995).
7. G. Holland, *ibid.* **54**, 2519 (1997).
8. A. Kattenberg *et al.*, in *Climate Change 1995: The Science of Climate Change*, J. T. Houghton *et al.*, Eds. (Cambridge Univ. Press, Cambridge, 1996).
9. Storm cases were selected from the northwest Pacific basin, because the global model's climatology of tropical storms appeared to be more realistic in that basin than in the western Atlantic. A fairly small selection region was used (8° to 26°N, 124° to 161°E) to help minimize differences in the track statistics between the control and high-CO<sub>2</sub> samples. This was done because a preliminary study of 20 cases showed that a relatively small sample of storms taken over a larger region could have substantial differences in track statistics as a result of the small sample size, which could lead to bias in the intensity comparisons. The strongest global model storm case for a particular pre-specified month and year was selected, with the sampling designed to spread the cases evenly over the 51 available years (one case per year) and across the calendar months of July through November.
10. S. Manabe, R. J. Stouffer, M. J. Spelman, K. Bryan, *J. Clim.* **4**, 785 (1991).
11. T. R. Knutson and S. Manabe, *ibid.*, in press.
12. The GFDL R30 global coupled ocean-atmosphere climate model has an atmospheric component with resolution of about 2.25° latitude (250 km) by 3.75°

longitude (400 km) and 14 vertical levels. Two 120-year experiments were done with the model: (i) a control integration with CO<sub>2</sub> constant at present-day levels and (ii) a transient CO<sub>2</sub> increase experiment in which atmospheric CO<sub>2</sub> levels increased at +1% per year compounded (that is, by a factor of 2.57 by year 95). Data from the years 70 to 120 of these two experiments provided the initial conditions and time-dependent boundary conditions for the regional model case studies.

13. A. J. Broccoli and S. Manabe, *Geophys. Res. Letters* **19**, 1525 (1992).
14. Y. Kurihara, R. E. Tuleya, M. A. Bender, *Mon. Weather Rev.*, in press.
15. The hurricane prediction system consists of an 18-level, triply nested, moveable mesh atmospheric model with a model-generated initial vortex. The outer grid covers a region 75° by 75° at a resolution of 1°, whereas the innermost grid covers a region 5° by 5° at a resolution of 1/6°, or about 18 km. The CO<sub>2</sub> level in the hurricane model was adjusted to the appropriate level for each particular case. As well as differing in spatial resolution, the global and regional models differ in model physics, diurnal variation, and so on.
16. M. A. Bender, R. J. Ross, R. E. Tuleya, Y. Kurihara, *Mon. Weather Rev.* **121**, 2046 (1993).
17. In the vortex replacement procedure, the case study storms from the global model were traced back for 2 to 4 days from the time of maximum intensity to an earlier stage of development (at least one closed-surface isobar, using a 4-mb contour interval). The global model storm—but not the background environmental flow fields—was then filtered out and replaced by a more realistic disturbance vortex as an initial condition. The replacement vortex was generated with the GFDL hurricane model's initialization scheme (16), using an identical target disturbance (maximum wind 17.5 m/s at a radius of 175 km) for each case. This procedure is analogous to that presently used for hurricane prediction at NCEP, except that in the operational case the disturbance target is based on actual storm observations and the global fields are derived from operational analyses.
18. S. Siegel and N. J. Castellani, *Nonparametric Statistics for the Behavioral Sciences* (McGraw-Hill, New York, ed. 2, 1988).
19. The one-sided two-sample KS test was implemented with the use of the Numerical Algorithms Group library routine G08CDF.
20. T. R. Knutson, R. E. Tuleya, Y. Kurihara, data not shown.
21. The available distribution for the tests at each hour consisted of cases that had not been screened out for that hour. We screened from each storm case sample any time periods in which the storm had been located over a major land mass within the past 6 hours or was located north of 30°N (where higher environmental vertical wind shear and lower SSTs are generally found). No attempt was made to exclude cases in which the primary storm interacted with another weather system.
22. Confidence intervals (95%) for the fifth strongest storm measure were estimated separately for each model integration hour on the basis of 10,000 random "bootstrap" resamples with replacement (23) of the available sample for that hour. Similar results were obtained using the fourth or sixth strongest storm.
23. B. Efron and R. Tibshirani, *Science* **253**, 390 (1991).
24. In order to minimize the imbalance between wind and mass fields in both the case study and the idealized approach, the surface pressure and the temperature fields were recomputed at the end of the vortex replacement procedure by solving a form of the reverse balance equation.
25. J. Lighthill *et al.*, *Bull. Am. Meteorol. Soc.* **75**, 2147 (1994).
26. We thank J. D. Mahlman for support and advice on our project; A. Broccoli, I. Held, and three anonymous reviewers for comments on the manuscript; and K. Emanuel and G. Holland for providing their MPI codes.

18 November 1997; accepted 13 January 1998